

**Wind regimes during the Last Glacial Maximum and early Holocene:
evidence from Little Llangothlin Lagoon, New England Tableland, eastern
Australia**

James Shulmeister

School of Geography, Planning and Environmental Management, University of Queensland, St
Lucia 4072 Queensland, Australia

** Corresponding author: Ph +61 7 334 61644. Email: james.shulmeister@uq.edu.au*

Justine Kemp

Australian Rivers Institute, Griffith University, Nathan 4111 Queensland, Australia

Kathryn E. Fitzsimmons *

Department of Human Evolution, Max Planck Institute for Evolutionary Anthropology,
Deutscher Platz 6, D-04103 Leipzig, Germany

Allen Gontz

School for the Environment, University of Massachusetts-Boston, Boston MA 02125, USA

Abstract

Here we present the results of a multi-proxy investigation, integrating geomorphology, ground penetrating radar and luminescence dating, of a high elevation lunette and beach berm in northern New South Wales, eastern Australia. The lunette occurs on the eastern shore of Little Llangothlin Lagoon and provides evidence for a lake high stand combined with persistent westerly winds at the Last Glacial Maximum (LGM - centring on 21.5 ka) and during the early Holocene (c. 9 and 6 ka). The reconstructed atmospheric circulation is similar to the present-day conditions and we infer no significant changes in circulation at those times, as compared to the present day. Our results suggest that the Southern Hemisphere westerlies were minimally displaced in this sector of Australasia during the latter part of the last ice age. Our observations also support evidence for a more positive water balance at the LGM and early Holocene in this part of the Australian sub-tropics.

Keywords

Westerlies, last glacial maximum (LGM), lunette, aeolian, lake levels, palaeolimnology, palaeohydrology, ground penetrating radar (GPR), optically stimulated luminescence (OSL)

1 Introduction

The temperate latitude westerly wind system influences the southern half of the Australian continent, and influences not only this region's climate but also the formation and response of its landscape systems. Understanding the history of the westerlies in the Australasian region is therefore important for understanding the climate and environmental history of eastern Australia (Shulmeister et al., 2004; Fletcher and Moreno, 2012; Lorrey et al., 2012).

Here we investigate past wind regime changes in eastern Australia as reflected in the shoreline marginal landforms of the Little Llangothlin Lagoon (LLL). LLL is a presently shallow lake which sits at 30 °S (30° 5' 9"S, 151° 46' 53"E) in northern New South Wales. It lies close to the present day northern boundary of the winter westerlies, therefore providing an excellent opportunity to investigate long-term changes in prevailing wind direction and intensity. The lagoon has a lunette (transverse shoreline dune) on its eastern shoreline and a possible beach berm on its south-eastern margin. These landforms reflect aeolian and wave-driven transport and deposition of sediments, and consequently provide indicators for the orientation of prevailing wind directions and intensity at the time of sediment deposition (Bowler, 1968; Bowler, 1973, 1983). In this study we undertook luminescence dating combined with geomorphic and stratigraphic investigations to reconstruct past periods of westerly, and possible north-westerly, prevailing wind flow in this region.

The endorheic basin was formed in gently undulating tableland comprising Tertiary basalt flows at approximately 1300 m above mean sea level (AMSL). The western shoreline of LLL is dominated by a low ridge of basalt, which rises 30 m above the lake (see Fig 1). On the eastern side of the basin, the lake is bound by a low hill of granite that forms part of the New England Batholith (Shaw and Flood, 1981). The Lagoon covers an area of 1.2 km² and has a catchment

of 3.2 km². LLL is a shallow, roughly circular permanent lake with a maximum depth of 2 m that shallows during droughts, which in this part of Australia are often associated with El Nino years. As far as we can determine, the lake has never dried out fully in post-European settlement times (Woodward et al., 2014b). Another, smaller, lake (Billy Bung Lagoon) lies c. 500 m to the southwest of LLL and is separated from the main lake by the low basalt ridge.

The origin of the New England ‘lagoons’ is cryptic. Conraeds (1989) showed that they were associated with former drainage lines that were occupied by basalt flows. He suggested that uneven infilling of former valleys by basalt during the Tertiary produced shallow depressions where the shallow lakes and swamps, locally called ‘lagoons’, formed. Similar lakes have been described elsewhere along the tablelands of the Great Dividing Range and Ollier (1979) suggested a tectonic origin for these features, proposing that uplift of the Eastern Highlands caused back tilting on many streams. Other authors such as Bell et al. (2008) have suggested a deflationary origin, where intense weathering occurred as a result of wetting and drying of the basalt. The mechanisms are not incompatible and deflation may have enhanced and maintained the basins which were created by back-tilting.

Many of these upland lakes have lunettes on their eastern margins (*sensu* Bowler 1976). These are transverse crescentic ridges dominated by wave action and shoreline drift, with coarse textured wave-built ridges on downwind margins (Bowler, 1986). Their regular outline reflects influence of strong wave action, while the aeolian deflation of sands from the beach forms foreshore dunes with an orientation equivalent to the winter wind resultant vector (Bowler, 1971). The proportion of clay and silt in lunettes increases during periods of shoreline regression, and is derived from efflorescence and pelletisation of saline lacustrine sediments on the drying lake floor.

The catchment is fed by summer rainfall (mean = 880 mm) and has a theoretical net annual moisture balance deficit of c. 400 mm (Woodward et al., 2014a). The regional vegetation is dominated by montane open eucalypt woodland, while the lagoon itself contains extensive beds

of tall spike rush *Eleocharis sphacelata* and the water plant *Potamogeton tricarinatus* in the deeper parts of the basin. Other swamp plants, including *Carex glaudichaudiana*, are dominant in the surrounding wet margins of the lagoon.

The lagoon has been intensively investigated from a palaeoecological and environmental viewpoint because it is a major bird reserve as well as a Ramsar wetland. Furthermore, the site has been identified as a location of exceptional soil erosion since European settlement (Gale et al., 1995; Gale and Haworth, 2005), although this has recently been challenged (Woodward et al., 2011). The site has more recently become a focus for work due to inferred changes to basin hydrology in response to tree clearance during European settlement of the New England Tablelands (Woodward et al., 2014a). There has also been some investigation of the archaeological history of the lagoon suggesting that landscapes such as these provided relatively rich resources for Aboriginal people, and that New England lagoons became the foci for ceremonial activities, although the degree to which hydrological conditions influenced human activity remains poorly understood since chronological control for the pre-European period has so far been lacking (Beck et al., 2015).

This paper examines the geomorphic context of shoreline features on the western and southern margins of the lagoon and focuses on the history of lake-margin sediment deposition to reconstruct the climatic circulation from the last glacial maximum (LGM) into the Holocene.

2 Materials and Methods

2.1 Field investigations

Transects across an apparent beach berm and the lunette were surveyed using a MALA ProEx ground penetrating radar (GPR) system with a 500 MHz antenna and integrated high-resolution GPS. The GPR data were collected in transects forming a rough grid parallel and perpendicular to the trend of hypothesised beach and lunette landforms. The GPR was hand-drag at a speed of ~ 4 kph and fired using time firing at a rate of 10 Hz resulting in an average along-track

resolution of 0.11 m and 0.07 m vertical resolution, based on a center frequency of 500 MHz. After acquisition, radar data were processed using GPR Slice software (DC drift; user-defined signal gain; bandpass lo=350 MHz, hi=650 MHz; background removal). Profiles were topographically corrected using elevation data from the GPS system and spot-checked using known elevations. While absolute topography was not reliable, relative elevation was consistently reproducible. Individual profiles were converted to depth-distance using the published radar velocity for wet sands of 0.07 m/ns in the beach ridges and dry sands 0.12 m/ns in the lunette (Neal, 2004). Depth-distance profiles were used to evaluate sediment thickness and observe true geometry of radar reflectors.

The sub-surface sediments were logged using a hand auger to a depth of between 0.6 m and 1.2 m, depending on sub-surface conditions. Sub-samples were collected for grain size analyses. Four samples were collected for optically stimulated luminescence (OSL) dating using steel tubes, wrapped in black plastic, and transported to the Max Planck Institute for Evolutionary Anthropology in Leipzig for analysis.

2.2 OSL dating - Equivalent dose measurements

Sample preparation and measurement for OSL dating was undertaken in the luminescence dating laboratory of the Department of Human Evolution, Max Planck Institute for Evolutionary Anthropology in Leipzig. The OSL samples were prepared under subdued red light using published methods (Fitzsimmons et al., 2014). This involved sieving, applying treatments to remove carbonates and organic matter, and isolating pure, 180-212 μm quartz grains. The outer ~ 10 μm alpha-irradiated rind of each grain was removed by etching in hydrofluoric acid, and the sample was then subjected to a final sieve to remove finer fragments which had broken off during etching. The quartz grains were then prepared as small aliquots (18 discs; 1 mm diameter) for preheat testing and as single grains (600 grains; 6 single grain discs) for equivalent dose (D_e) measurement.

D_e measurements were undertaken using an automated Risø TL-DA-15 equipped with blue light-emitting diodes (for preheat and initial dose estimate testing), and a TL-DA-20 reader with a

single grain attachment containing a green laser emitting at 532 nm, for light stimulation of single aliquots and single grains respectively (Botter-Jensen et al., 2000). Irradiation was provided by calibrated $^{90}\text{Sr}/^{90}\text{Y}$ beta sources. Equivalent doses were determined on single grains using the single aliquot regenerative dose (SAR) protocol of Murray and Wintle (2000; 2003). Preheat temperatures of 260°C were chosen based on the results of the preheat plateau tests (Figure S1) for the natural and regenerative doses, with a preheat temperature of 220°C for the test doses (0.94 Gy).

Individual grains were analysed for their suitability for OSL dating based on the selection criteria of Jacobs and Roberts (2007). The single grain dose distributions of all samples are >40% overdispersed with complex dose populations (Table S1), and therefore the Finite Mixture Model (FMM) was used to identify dose populations (Galbraith and Green, 1990). The OSL dating results are summarised in Table 1. Equivalent dose distributions for the four samples are shown as radial plots, with the FMM-derived dose populations highlighted, in Figure S4.

2.3 OSL dating - Dose rate calculations

Uranium, thorium and potassium (^{40}K) activities were measured in the “Felsenkeller” laboratory at VKTA Rossendorf in Dresden, Germany, using low-level gamma-ray spectrometry. Dose rates were calculated using the conversion factors of Stokes et al. (2003) with β -attenuation factors taken from Mejdahl (1979). Beta counting was based on 1 g homogenized subsamples and used for the beta component of the dose rate. Measured water contents ranged from 5-10% and these values were used for all samples. Cosmic dose rates were calculated from Prescott and Hutton (1994).

3 Results

3.1 Geomorphology

There are no dune or beach deposits on the western side of the lake (Figure 1). The main geomorphic feature on the eastern side of the lake is can you show this on figure 1? a small dune system and the low basalt ridge. The dunefield comprises a north-south oriented ridge less than 2 m high adjacent to the

lake, a swale behind that is occupied by a small stream and a small sand flat area that extends up to 50 m east of the lake shore. is 'dune system' the correct term? I imagined a field of multiple dunes but perhaps you are just referring to the lunette?

The lunette on the eastern shore is composed of poorly sorted medium sand grading upwards into fine sand with accessory silt contents of 3-15%. Particle size results and other stratigraphic information are plotted on Figure 1. GPR transects are shown in Figures 2a and 2b.

Please add some PSD data in the supplementary data.

On the SE margin of LLL, there is a partly infilled outlet, immediately to the west of which is a c. 100 m long, 50 m wide low (< 1m) berm. The berm is poorly to well sorted, medium and coarse quartz rich sand with iron-manganese, pisolithic gravel and a silt content of 1-14%.

again, please add to supplementary data

3.2 GPR results

The GPR proved effective at mapping stratigraphic architecture and subsurface character to a depth shallower than 4 m in the berm (Figures 2a and 2b). GPR data suggest the presence of several distinct units related to changes in lake level and the development of spit/barrier and berm formations (Shan et al., 2015; Thompson et al., 2011). The berm showed strong internal stratification on feature perpendicular lines with strong sigmoidal clinoforms indicating beach progradation to the west (Thompson et al., 2011) as well as low-angle sub-parallel reflectors dipping to the east suggesting basin infill via over wash processes. This package is underlain by a hyphenate convex up package of reflections that are sub-parallel with dips to the east and west. Comparision of this feature with those identified by Shan and others (2015) suggest the complex in underlain by a spit complex. Additional information on the character of the lower units associated with the interpreted spit are unavailable due to the existing GPR data coverage.

please indicate the spit unit(s) on the GPR interpreted transects. I had difficulty working out which they were.

The internal stratigraphy of the fine-grained lunette was difficult to assess with the GPR. Evidence of extensive modern bioturbation by rabbits was observed during the radar acquisition. The shallow penetration did however show weak internal characteristics commonly associated with lunette formation (Thomas and Burrough, in press). These included eastward dipping high angle reflectors that are truncated on the western facing slope, coupled with areas of parallel to

you need to say that this data is not shown (at least, that's what I understood). Could this be added to the supplementary data?

sub-parallel reflections that change to steeply dipping reflections. All reflectors are laterally discontinuous and show evidence of disturbance at all depths observed, rendering the GPR data ineffective at determining genetic processes or detailed landform characteristics.

3.3 OSL results

The OSL age data are summarised in Table 1, and shown with respect to stratigraphy and catchment geomorphology in Fig 1. The three samples collected from three different locations along the lunette suggest that the entire landform was formed during the LGM, between c. 24-19 ka. The secondary age populations identified by FMM are all younger than the main phase of deposition (Figure S2) and suggest phases of partial reactivation or pedogenic infiltration of material into the lunette. The younger age populations from sites LL3 and LL4 in the central part of the lunette are comparable and suggest contemporaneous post-depositional infiltration of younger material or partial reactivation of the lunette in the early Holocene (c. 9-8 ka; Table S2). Sample L-EVA 1230 (LL3) exhibits a third peak centred on 11.8 Gy (9.1 ka). The second major age population from the LL2 site in the southern part of the lunette dates to the mid-Holocene (5.6 ± 0.5 ka; Table S2) and suggests spatial and temporal variability in the Holocene post-depositional pedogenesis (or reactivation) of the lunette.

The overdispersion on individual D_e results from the berm was too high (79.9%; Table S1) to reliably define a depositional age, although the largest age population yields a mid-Holocene age (5.1 ± 0.5 ka; Table 1) comparable with the reactivation of the southern part of the lunette at LL2. The minor dose populations yield ages of 11.1 ± 1.6 ka, 2.3 ± 0.3 ka and 1.2 ± 0.1 ka (Table S2).

4 Discussion

4.1 A possible spit/barrier berm on the SE corner of the lagoon

Figure 1 does not show any other feature except the 'sand and gravel berm'. Is that what you mean? If it is, then use the term here to avoid confusion and then tell us why you reached that conclusion.

The most cryptic landform in the basin is the **barrier feature on the SE margins** of LLL. The feature was identified by Gale et al. (2005), who interpreted it as part of a relict older lunette feature. From visual observations alone, this is a reasonable interpretation because the low berm does look like the erosional shadow of an older ridge. Our sedimentologic and GPR structural investigations, however, discount this interpretation. Based on both GPR and field observations from pits, the feature is a beach berm, with numerous small wash-over structures (see Fig. 2a).

The berm barrier feature is composed of pea sized gravels with a finer sandy matrix. We assume the sandy matrix to be post-depositional because it is incompatible with the sedimentary structures and post-depositional infilling of openwork deposits is common. In addition, the contrast between locally sourced detrital basalt gravels and reworked quartz-rich sand and silt is striking. The matrix may have accumulated either through aeolian accretion, or through filtration of sands through the barrier during high lake stands when the berm would have acted as a permeable filter for the lake. Given the mostly coarse nature of the matrix (medium to coarse sand), we prefer the two-stage filtration hypothesis.

The pea-sized gravels are detrital. We suggest that the most likely origin for this feature is as a spit that developed from the basalt ridge on the SW edge of the lake, and that the basalt gravels were moved along the shoreline by longshore drift. The barrier ultimately cut off an area to the SW of the present lake that was part of a larger, ancestral lake feature, for which we have no age constraint due to the lack of associated sedimentary deposits. The luminescence sample based on the finer matrix material yielded a highly dispersed dose distribution with four age populations, which is not unexpected given our hypothesis that the matrix is post-depositional. The grains may represent the accretion of fines to the barrier during high stands in the lake in the early (c. 11 ka), mid (c. 5.6 ka) and late Holocene (c. 2.3 ka, 1.2 ka).

4.2 Aeolian history of LLL from the lunette

Based on the morphology, sedimentary composition and internal structure, the feature along the eastern shoreline of LLL is clearly a composite beach and aeolian landform. The quartz-rich

sands were most likely derived from the granites on the eastern side of the catchment, which deposited into the lake and were subsequently reworked onto the shoreline. Curiously, even though half the basin is comprised of basalt, there is little evidence for basalt-derived sediments in the lunette system. By contrast, the fine sediments in the depocentre of the lake basin are primarily derived from basalt (e.g. Woodward et al., 2011). This implies that there is an effective sorting mechanism within the basin. The obvious candidate for this process is wind-blown waves.

Present day wind roses for LLL (BOM, 2014) demonstrate that there are two primary wind directions (Figure 4), one from the east and the other from the west to north-west. These prevailing winds have strong seasonal components. Winter winds (August) are dominated by westerlies and provide the strongest and most persistent flows (8% calm) consistent with eastward transport and deposition of sediments onto a lunette situated on the eastern shoreline of LLL. Summer winds (February) are dominated by easterlies associated with onshore circulation on the northern limb of the sub-tropical high pressure cell in summer (Fig. 4). These easterly winds are on average weaker (20% calm) but do include short periods of relatively high intensity winds which might be expected to result in sediment transport to, and deposition onto, the western side of the lake. It is curious therefore that all depositional landforms marginal to LLL are located on the east and south-east sides of the lake, with no deposition on the western shoreline. This indicates that the most effective net sand-transporting wind, associated with lunette and berm formation, was from the west/north-west. The transport is most likely to have been primarily sub-aqueous, since the relatively poor sorting in the foredune indicates only intermittent aeolian transport, at least of the coarsest component.

you could calculate the potential sand drift direction using Fryberger's method.
given the short distances involved, parent material, and small catchment I think that poorly sorted aeolian deposits are entirely understandable.

One obvious question is why the westerlies are so strongly recorded in the LLL lunette, and not the easterlies. This partly reflects the greater frequency of high wind speeds from the west, but on its own it is unlikely to explain the entire phenomenon. The most parsimonious answer integrates the sedimentary information with seasonal variations in the biological system. The rush beds occurring in the shallower parts of the lake are most fully developed during the summer. Unlike much of Australia, winters are severe on the New England Tablelands due to the

relatively high elevations, and seasonal die-back of the jointed wire rush is also observed today. New growth emerges in spring and dies off in autumn in cooler, high altitude sites (Rajapaskse et al., 2006). Consequently, the summer peak in vegetation cover disrupts the wind fetch over the lake precisely at the same time as the easterly winds penetrate the tablelands, thereby reducing the ability for waves to set up during the warmer months.

The luminescence ages from the lunette are coherent; all three samples are dominated by grains that are LGM in age. The samples all overlap at 2σ and produce a mean age of 21.5 ka, indicating that the main phase of dune activity at LLL occurred during the LGM. Our interpretation that the dominant sediment transport mechanism was subaqueous therefore implies

that the LGM oversaw permanent, and probably full, lake conditions at LLL. Evidence from pollen records and sedimentary archives from the depocentre of the lake support our hypothesis for a full lake during the late LGM (c. 19 ka). Our argument for the persistence, and perhaps

intensification, of winter westerlies throughout the LGM at LLL is also confirmed by observations made at North Stradbroke Island some 300 km to the north-northeast of our site (Petherick et al., 2009; McGowan et al. 2009). North Stradbroke Island lies at the very northern edge of the westerlies zone, and the accession of fine aeolian material into a dune lake there indicates that the winter westerlies were operative at the LGM in South East Queensland at 27.20°S (Petherick et al., 2009; McGowan et al. 2009).

Further south there are several records (of varying quality) showing high lake levels at the LGM; Lake Urana, Lake George (?), Wangoom etc.

A secondary peak in grain ages is observed from all three lunette samples. This peak is less well defined but in all three cases relates to the early to mid-Holocene between 9 and 6 ka. Work from the lake (Woodward et al., 2011) has already demonstrated that the early Holocene was the last phase, before the modern anthropogenically modified lake, with lake-full conditions as represented by extensive *Eleocharis* beds. We infer partial reactivation at this times.

Unless you provide a PDF (or similar), this is not substantiated.
But what is the deposition mechanism which allows inclusion of these grains at depth? Illuviation? How could you differentiate it from bioturbation, for example? There is insufficient explanation of the geomorphic and pedogenic processes and alternatives.
show us a PDF

We note a third grain age peak in one lunette sample (EVA1230) at c. 3 ka. This is both the weakest individual age peak and not replicated at any other site. It is possible that this represents a dune re-activation event, bioturbation, or even aboriginal usage of the site which has been proposed to have intensified during the late Holocene (post 4300 yr; Beck et al., 2015). At this

surely you have to support this with a citation or explanation (or, even better, both)

whereas they are not today?

330 stage this event, if real, is still poorly controlled chronologically and we do not interpret it
331 further.

332
333 Overall, our evidence demonstrates that at the LGM, winter westerly winds were strong enough
334 to form the eastern shoreline lunette in a single phase, with possible later reactivation during the
335 early Holocene. Critically, ^{foredune}~~dune~~ activation depends as much on high water levels in the lake as it
336 does on sand mobilizing winds (Bowler, 1983). During the Pleistocene, elevations above 800 m
337 in the region were subject to extensive, active development of block deposits, screes, and
338 solifluction lobes, indicating winter cooling of at least 10.5 °C relative to present (Slee and
339 Shulmeister, 2015). Reduced evaporation at this time is likely to have been sufficient to cause
340 the change to a positive hydrological balance in the lake.

341 ^{see also Hesse et al. 2003 Quat Intl for LGM sand dunes in the Blue Mts and discussion of conditions necessary to allow aeolian activity}

342 For the intervening periods at least in the Holocene, the evidence (Woodward et al., 2014a)
343 suggests that water levels were lower and/or even that the lake was ephemeral. It is highly
344 unlikely that sand would be transported to the high stand beach during low lake levels. If the
345 entire basin floor fully dried out, pelletised clays might be expected, and yet none are observed.
346 There are two likely reasons for this. Firstly, this high elevation site is unlikely to become very
347 arid even during dry phases when swampy conditions probably persisted on the basin floor.
348 Similarly, it is unlikely that salt formation is significant in this setting and clay pelletisation may
349 not occur. This is similar to observations from Lake George, which also occurs in a cool
350 temperate climate setting along the Dividing Range (Fitzsimmons and Barrows, 2010).

351 ^{see also Page et al 1996 JQS for a clay free lunette at the LGM but at low altitude}

352 In summary, these records strongly suggest that for the two intervals recorded (the LGM and
353 early Holocene), the overall circulation conditions at LLL were very similar to the present day.
354 This region presently lies near the northern limit of westerly penetration in winter. Westerlies
355 occurred during both the early Holocene and the LGM ^{suggesting that at both time intervals the}
356 ^{position of the westerly jet lay near 30°S,} which is its modern track. For the intervening periods,
357 absence of evidence is not evidence of absence and if the winter westerly lay at this latitude
358 during peak warming in the early Holocene and during the LGM, it seems reasonable to suppose
359 that this track has been persistent over the last 25 ky.

Reinfelds et al
2015 have given a
sound argument
for why lower
temperatures should
result in more
runoff and,
presumably, favour
higher lake levels

This cannot be
determined from a
single site (where
no change has
been found). The
posiiton of the jet
cannot be
determined from
surface westerlies.
There is a
confusion of terms
or concepts.

One possibility is that the westerly lay north of its current track during the LGM and that the timing of the westerlies at LLL shifted seasonally. A northward shift of $\sim 3^\circ$ (350 km) in the position of the westerly wind belt during MIS 2 was recorded in sediments from marine cores in the Tasman Sea (Hesse, 1994). Analysis of the aeolian component of lake sediments on North Stradbroke Island at 27°S for the period 25-22 ka indicates dust sources in the SW Murray-Darling Basin, with a secondary component from WNW of the site (Petherick et al. 2009). This lends support to a possible northward shift in the westerlies.

Conclusions

This study indicates that westerly winds constructed a foredune ridge at LLL during the LGM under the influence of high lake levels. This ridge was reactivated during high lake stands in the early to mid-Holocene. The persistence of westerly winds at this site during the LGM confirms observations from North Stradbroke Island at the northern limits of penetration of the temperate latitude westerlies. This suggests that the overall circulation pattern in this part of eastern Australia, at the modern northern limits of westerly winter flow, remained constant during both the LGM and the early Holocene. Overall, this points to minimal change in circulation patterns over the last 25 ky.

Team List

James Shulmeister

Justine Kemp

Kathryn Fitzsimmons

Allen Gontz

Copyright Statement

Except where explicitly acknowledged the authors hold the copyright of the materials presented.

Author Contributions

J Shulmeister lead the project, assisted with field sampling for OSL and grain size and lead the manuscript development. J Kemp assist in the field with OSL sample acquisition, conducted grain size analysis and participated in manuscript development. K Fitzsimmons oversaw the OSL sample analysis and participated in manuscript development. A Gontz lead the GPR acquisition and processing, assisted with OSL sampling and manuscript development.

Acknowledgements

This research was funded by an Australian Research Council Discovery Grant DP110103081, “The last glaciation maximum climate conundrum and environmental responses of the Australian continent to altered climate states”. We thank S. Hesse for assistance with OSL sample preparation. C. Woodward, J. Chang, and A. Slee assisted with fieldwork. We thank NSW Parks and Wildlife Service for access to the site and the local farmers for retrieving our vehicle from the bottomless suck hole!

References

- Bell, D.M., Hunter, J.T., and Haworth, R.J.: Montane lakes (lagoons) of the New England tablelands bioregion, *Cunninghamia*, 10, 475-492, 2008.
- Beck, W., Haworth, R., and Appleton, J.: Aboriginal resources change through time in New England upland wetlands, south-east Australia, *Archaeol Ocean*. 50, 47-57, 2015.
- Botter-Jensen, L., Bulur, E., Duller, G.A.T., and Murray, A.S.: Advances in luminescence instrument systems, *Radiat Meas*, 32, 523-528, 2000.
- Bowler, J.M.: Aridity in Australia: age, origins and expression in aeolian landforms and sediments, *Earth Sci Rev*, 12, 279-310, 1976.
- Bureau of Meteorology. Summary statistics Guyra Hospital. Climate Data Online. 2014. Available at: http://www.bom.gov.au/climate/averages/tables/cw_056229.shtml. Last accessed. 29 February, 2016.
- Coenraads, R.R.: Evaluation of the natural lagoons of the Central Province, NSW—Are they sapphire-producing maars?, *Explor Geophys*, 20, 347-363, 1989.

419 Fitzsimmons, K.E., and Barrows, T.T.: Holocene hydrologic variability in temperate
 420 southeastern Australia: An example from Lake George, New South Wales, *The Holocene* 20,
 421 585-59, 2010.

422 Fitzsimmons, K.E., Stern, N., and Murray-Wallace, C.V.: Depositional history and archaeology
 423 of the central Lake Mungo lunette, Willandra Lakes, southeast Australia, *J Archaeol Sci* 41, 349-
 424 364, 2014.

425 Fletcher, M.S., and Moreno, P.I.: Have the Southern Westerlies changed in a zonally symmetric
 426 manner over the last 14,000 years? A hemisphere-wide take on a controversial problem,
 427 *Quaternary Int*, 253, 32-46, 2012.

428 Galbraith, R.F., and Green, P.F.: Estimating the component ages in a finite mixture, *Nucl Tracks*
 429 *Rad Meas* 17, 197-206, 1990.

430 Gale, S.J., Haworth, R.J., and Pisanu, P.C.: The ²¹⁰Pb chronology of late Holocene deposition
 431 in an eastern Australian lake basin, *Quaternary Sci Rev*, 14, 395-408, 1995.

432 Gale, S.J., and Haworth, R.J.: Catchment-wide soil loss from pre-agricultural times to the
 433 present: transport-and supply-limitation of erosion. *Geomorphology*, 68, 314-33, 2005.

434 Haworth, R.J., Gale, S.J., Short, S.A., and Heijnis, H.: Land use and lake sedimentation on the
 435 New England tablelands of New South Wales, Australia, *Aust Geogr*, 30, 51-73, 1999.

436 Hesse, P.P.: The record of continental dust from Australia in Tasman Sea sediments, *Quaternary*
 437 *Sci Rev*, 13, 257-72, 1994.

438 Jacobs, Z., and Roberts, R.G.: Advances in optically stimulated luminescence dating of
 439 individual grains of quartz from archeological deposits, *Evol Anthropol*, 16, 210-223, 2007.

440 Lorrey, A.M., Vandergoes, M., Almond, P., Renwick, J., Stephens, T., Bostock, H., Mackintosh,
 441 A., Newnham, R., Williams, P.W., Ackerley, D., and Neil, H.: Palaeocirculation across New
 442 Zealand during the last glacial maximum at ~ 21 ka, *Quaternary Sci Rev*, 36, 189-213, 2012.

443 McGowan, H.A., Petherick, L.M., and Kamber, B.S.: Aeolian sedimentation and climate
 444 variability during the late Quaternary in southeast Queensland, Australia, *Palaeogeog*, *Palaeocl*,
 445 265, 171-81, 2008.

446 Mejdahl, V.: Thermoluminescence dating: beta-dose attenuation in quartz grains, *Archaeometry*
 447 21, 61-72, 1979.

448 Murray, A.S., and Wintle, A.G.: Luminescence dating of quartz using an improved single-aliquot
 449 regenerative-dose protocol, *Radiat Meas*, 32, 57-73, 2000.

450 Murray, A.S., and Wintle, A.G.: 2003. The single aliquot regenerative dose protocol: potential
451 for improvements in reliability, *Radiat Meas*, 37, 377-381, 2003.

452 Neal, A.: Ground penetrating radar and its use in sedimentology: principles, problems and
453 progress, *Earth Sci Rev*, 66, 261-330, 2004.

454 Ollier, C.D.: Evolutionary Geomorphology of Australia and Papua: New Guinea, *T I Brit Geog*,
455 4, 516-39, 1979.

456 Petherick, L.M., McGowan, H.A., and Kamber, B.S.: Reconstructing transport pathways for late
457 Quaternary dust from eastern Australia using the composition of trace elements of long traveled
458 dusts, *Geomorphology*, 105, 67-79, 2009.

459 Prescott, J.R., and Hutton, J.T.: Cosmic ray contributions to dose rates for luminescence and
460 ESR dating: Large depths and long term variations, *Radiat Meas*, 23, 497-500, 1994.

461 Rajapakse L., Asaeda, T., Williams, D., Roberts, J., and Manatunge, J.: Effects of water depth
462 and litter accumulation on morpho-ecological adaptations of *Eleocharis sphacelata*, *Chem Ecol*,
463 22, 47-57, 2006.

464 Shan, X., Yu, X., Clift, P.D., Tan, C., Jin, L., Li, M, and Li, W.: The ground penetrating radar
465 facies and architecture of a paleo-spit from Huangqihai Lake, North China: implications for
466 genesis and evolution, *Sediment Geol*, 323, 1-14, 2015.

467 Shaw, S.E., and Flood, R.H.: The New England Batholith, eastern Australia: geochemical
468 variations in time and space, *J Geophys Res-Sol Ea*, 86, 10530-10544, 1981.

469 Shulmeister, J., Goodwin, I., Renwick, J., Harle, K., Armand, L., McGlone, M.S., Cook, E.,
470 Dodson, J., Hesse, P.P., Mayewski, P., and Curran, M.: The Southern Hemisphere westerlies in
471 the Australasian sector over the last glacial cycle: a synthesis, *Quaternary Int*, 118, 23-53, 2004.

472 Slee, A., and Shulmeister, J.: The distribution and climatic implications of periglacial landforms
473 in eastern Australia, *J Quaternary Sci*, 30, 848-58, 2015.

474 Stokes, S., Ingram, S., Aitken, M.J., Sirocko, F., Anderson, R., and Leuschner, D.: 2003.
475 Alternative chronologies for Late Quaternary (Last Interglacial–Holocene) deep sea sediments
476 via optical dating of silt-sized quartz, *Quaternary Sci Rev*, 22, 925-941, 2003.

477 Thomas, D.S.G., and Burrough, S.L.: Luminescence-based chronologies in southern Africa:
478 analysis and interpretation of dune database records across the subcontinent, *Quaternary Int*, 1-
479 16, in press.

480 Thompson, T.A., Lepper, K., Endres, A.L., Johnston, J.W., Baedke, S.J., Argyilan, E.P., Booth,
 481 R.K., and Wilcox, D.A.: Mid Holocene lake levels and shoreline behaviour during the Nipissing
 482 phase of the upper Great Lakes at Alpena, Michigan, USA, *J Great Lake Res*, 37, 567-576, 2011.

483 Woodward, C., Chang, J., Zawadzki, A., Shulmeister, J., Haworth, R., Collecutt, S., and
 484 Jacobsen, G.: Evidence against early nineteenth century major European induced environmental
 485 impacts by illegal settlers in the New England Tablelands, south eastern Australia, *Quaternary*
 486 *Sci Rev*, 30, 3743-3747, 2011.

487 Woodward, C., Shulmeister, J., Bell, D., Haworth, R., Jacobsen, G., and Zawadzki, A.: A
 488 Holocene record of climate and hydrological changes from Little Llangothlin Lagoon, south
 489 eastern Australia, *The Holocene*, 6:0959683614551218, 2014a.

490 Woodward, C., Shulmeister, J., Larsen, J., Jacobsen, G.E., and Zawadzki, A.: The hydrological
 491 legacy of deforestation on global wetlands, *Science*, 346, 844-7, 2014b.

492
 493

Tables

Table 1. Equivalent dose (D_e), dose rate data and OSL age estimates for Lake Little Llangothlin. Dose rates are listed as attenuated based on published factors (Stokes et al. 2003; Mejdahl 1979).

Sample	D_e (Gy)	K (%)	Th (ppm)	U (ppm)	Beta dose rate (Gy/ka)	Cosmic dose rate (Gy/ka)	Water content (%)	Total dose rate (Gy/ka)	Age (ka)
L-EVA 1228 (LL1)	6.1±0.6	0.53±0.02	4.0±0.2	1.3±0.1	0.6±0.1	0.19±0.02	10±3	1.21±0.07	5.1±0.5
L-EVA 1229 (LL2)	19.2±0.4	0.34±0.02	3.5±0.2	1.3±0.1	0.5±0.1	0.18±0.02	5±3	1.02±0.06	18.9±1.2
L-EVA 1230 (LL3)	26.9±0.9	0.69±0.04	3.0±0.1	1.3±0.1	0.7±0.1	0.18±0.02	7±3	1.30±0.08	20.6±1.4
L-EVA 1231 (LL4)	22.9±1.2	0.56±0.02	2.7±0.1	0.7±0.1	0.5±0.1	0.18±0.02	6±3	0.98±0.05	23.4±1.8

Figure Legends

Figure 1. Geomorphology and sediments at Little Llangothlin Lagoon (30° 5' 9"S, 151° 46' 53"E), 18 km NE Guyra, NSW, showing the locations of GPR transects, sediment cores (right) and the position of OSL samples.

Figure 2a. GPR transects over the “berm”. See Fig 1. for location of transect. GPR line A7 was acquired perpendicular to the shoreline starting just lakeward of the highest point on the berm. Internal structures are characteristic of an interfingering beach-washover-basin fill sequence over a spit complex. Upper panel, raw data; lower panel, interpretation.

Figure 2b. GPR line A9 was acquired from the lake shore to the highest point on the berm. Internal structures show characteristics of a beach environment over a spit complex. Top left panel, raw data; top right panel, interpretation. The lower panel shows a conceptual model based on composite GPR profiles suggesting a lower lake facies with spit facies underlying beach, washover and basin fill facies.

Figure 3. Equivalent dose distributions for the LLL samples, illustrated as radial plots. The shaded populations in each case represent the dominant age peaks; the lines illustrate the other identified populations.

Figure 4. Rose of 9am wind direction vs wind speed in km/hr at Guyra Hospital, 1332 m AMSL (Bureau of Meteorology, 2014).

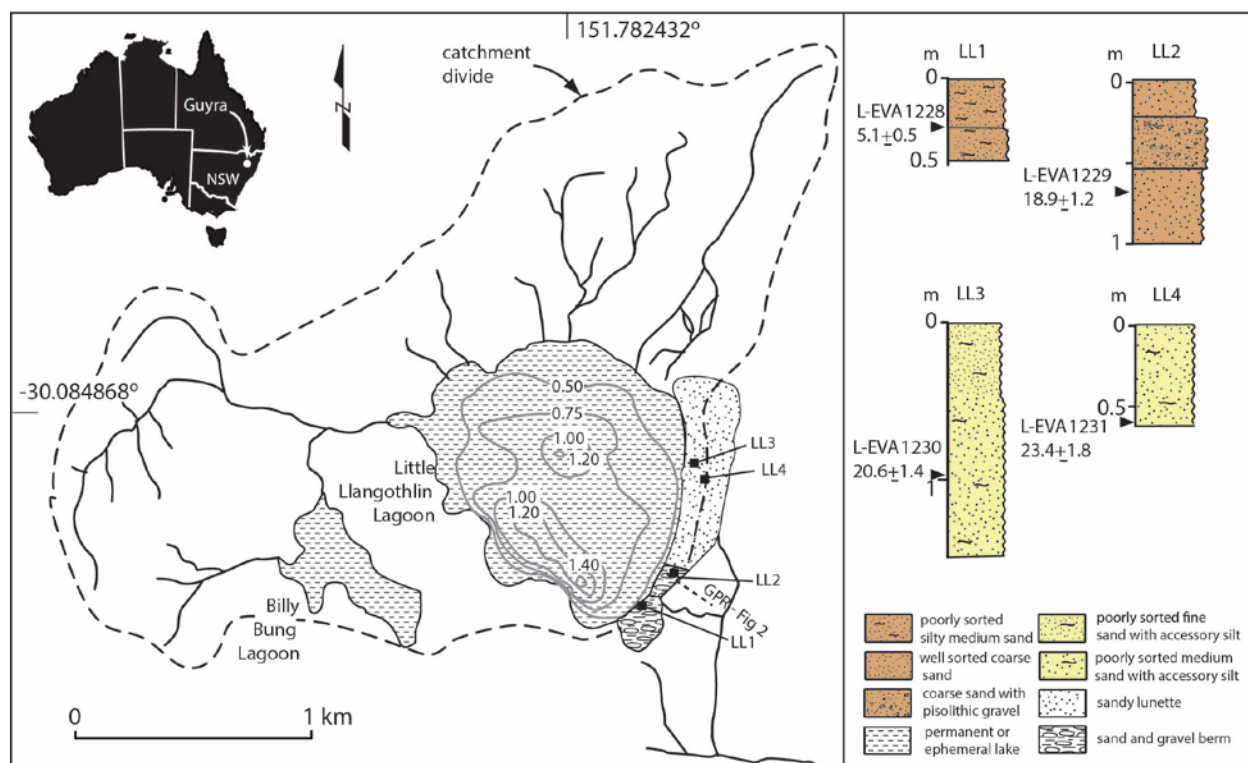
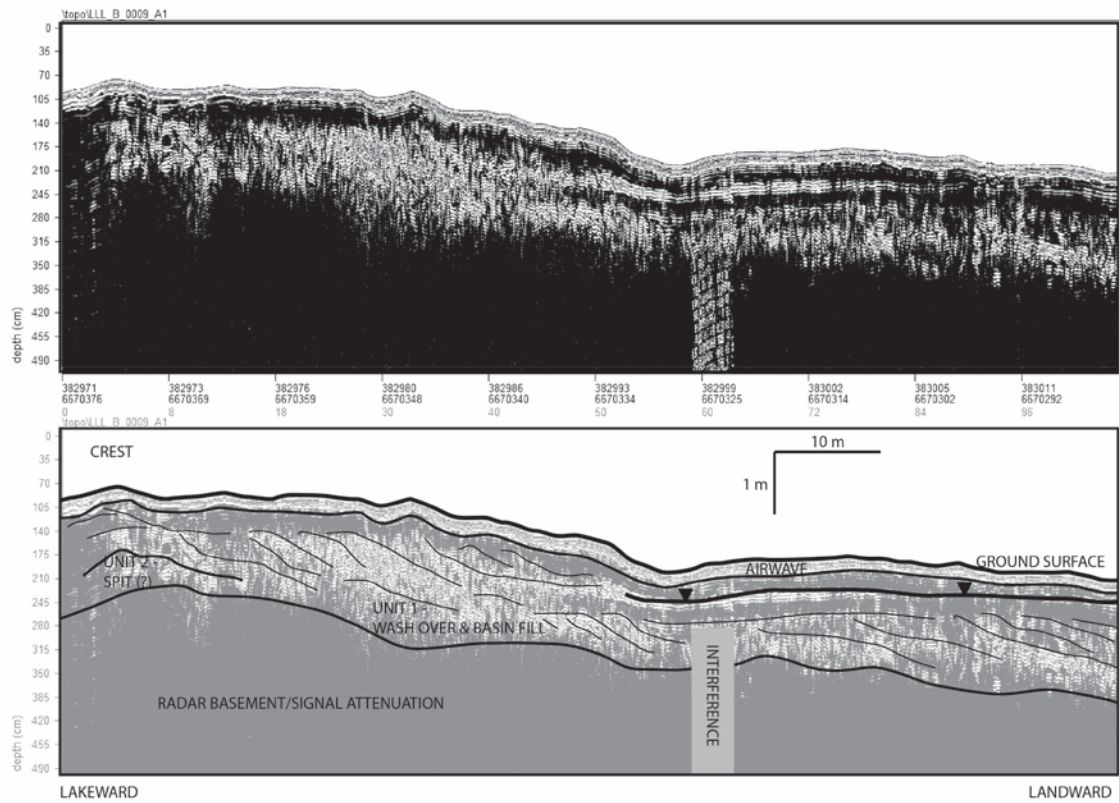


Figure 1



521
522 **Figure 2a**

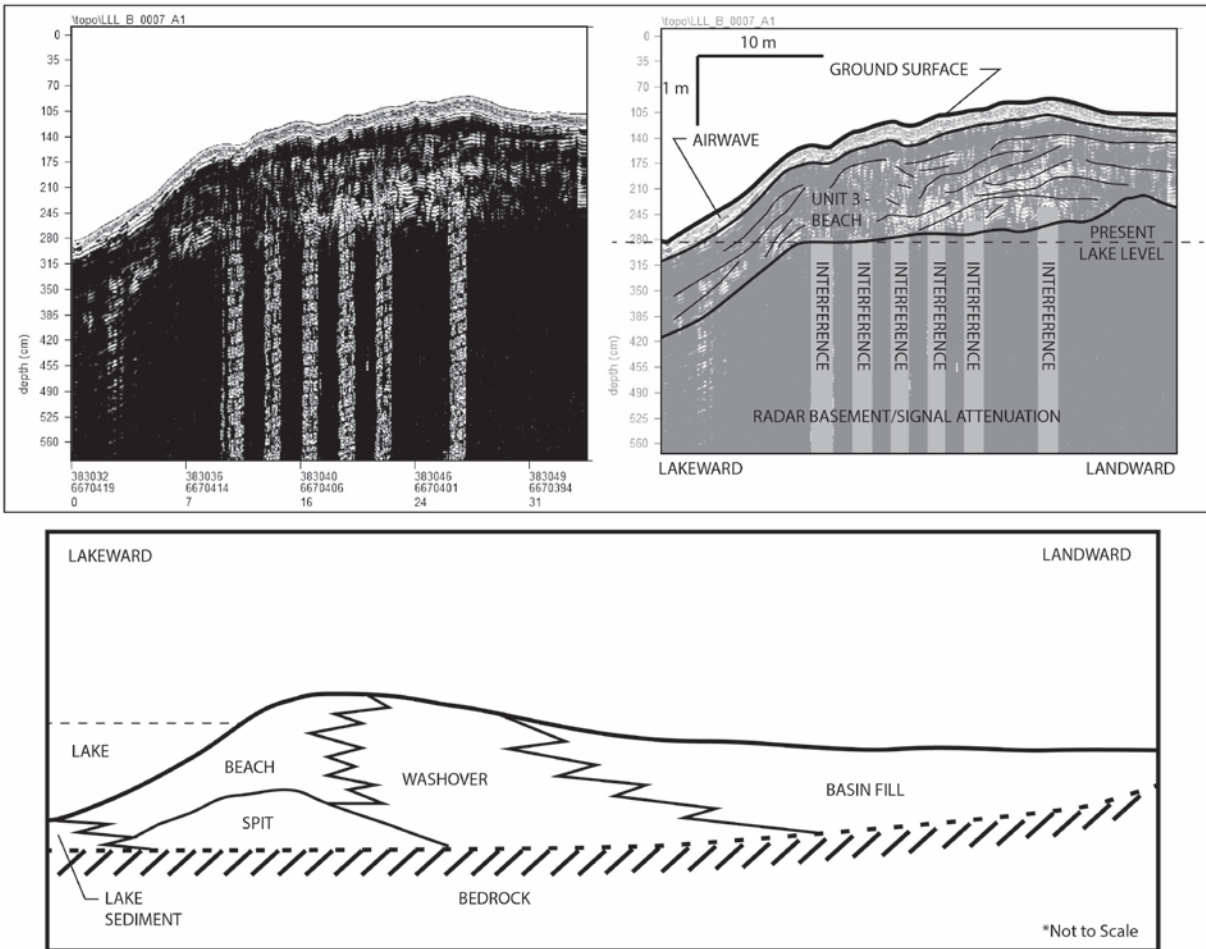


Figure 2b

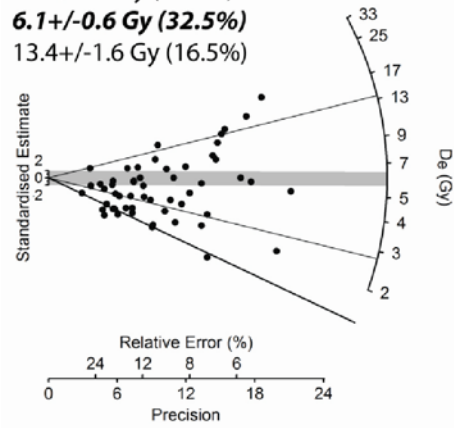
EVA1228:

1.4+/-0.1 Gy (22.4%)

2.8+/-0.3 Gy (28.7%)

6.1+/-0.6 Gy (32.5%)

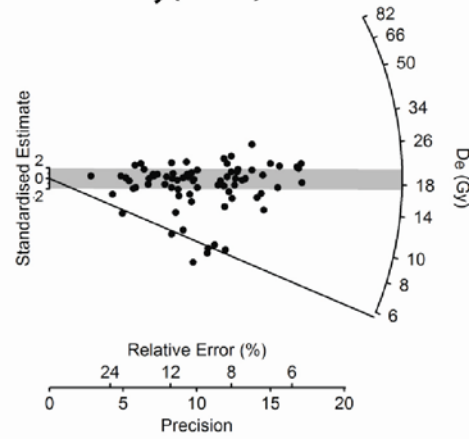
13.4+/-1.6 Gy (16.5%)



EVA1229:

5.7+/-0.3 Gy (12.8%)

19.2+/-0.4 Gy (87.2%)

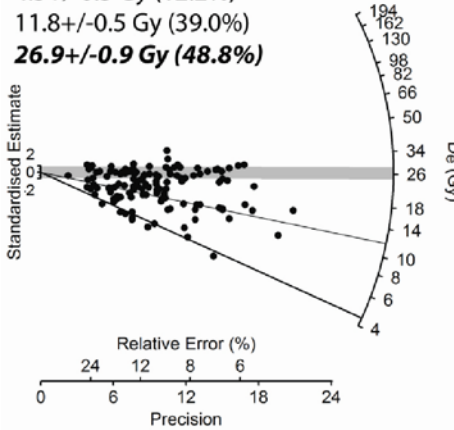


EVA1230:

4.5+/-0.3 Gy (12.2%)

11.8+/-0.5 Gy (39.0%)

26.9+/-0.9 Gy (48.8%)



EVA1231:

7.8+/-0.5 Gy (43.2%)

22.9+/-1.2 Gy (56.8%)

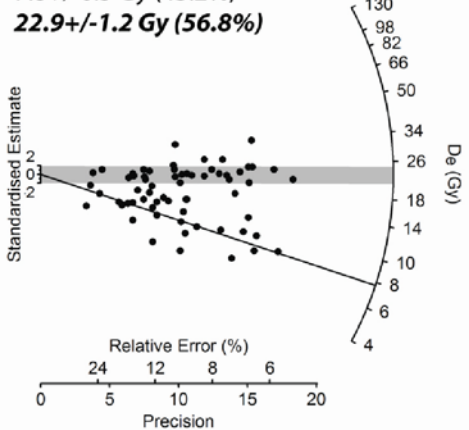


Figure 3

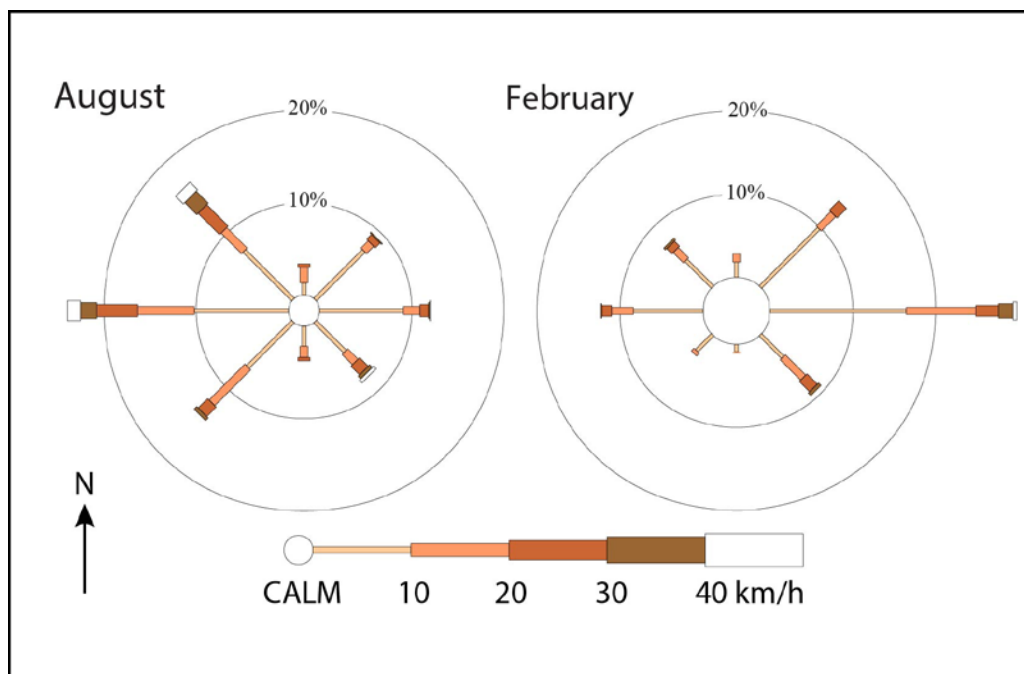


Figure 4